

Is There a Detectable Vishniac Effect?

Evan Scannapieco

Departments of Physics and Astronomy, University of California, Berkeley, CA 94720-7304

ABSTRACT

The dominant linear contribution to cosmic microwave background (CMB) fluctuations at small angular scales ($\lesssim 1'$) is a second-order contribution known as the Vishniac or Ostriker-Vishniac effect. This effect is caused by the scattering of CMB photons off free electrons after the universe has been reionized, and is dominated by linear perturbations near the $R_V = 2 \text{ Mpc}/(h\Gamma/0.2)$ scale in the Cold Dark Matter cosmogony. As the reionization of the universe requires that nonlinear objects exist on some scale, however, one can compare the scale responsible for reionization to R_V and ask if a linear treatment is even feasible in different scenarios of reionization. For an $\Omega_0 = 1$ cosmology normalized to cluster abundances, only $\sim 65\%$ of the linear integral is valid if reionization is due to quasars in halos of mass $\sim 10^9 M_\odot$, while $\sim 75\%$ of the integral is valid if reionization was caused by stars in halos of $\sim 10^6 M_\odot$. In Λ or open cosmologies, both the redshift of reionization and z_V are pushed further back, but still only $\sim 75\%$ to $\sim 85\%$ of the linear integral is valid, independent of the ionization scenario. We point out that all odd higher-order moments from Vishniac fluctuations are zero while even moments are non-zero, regardless of the gaussianity of the density perturbations. This provides a defining characteristic of the Vishniac effect that differentiates it from other secondary perturbations and may be helpful in separating them.

Subject headings: cosmic background radiation – cosmology: theory

1. Introduction

While recombination at $z \approx 1100$ marked the end of ionized hydrogen from the viewpoint of a linearly evolving universe, the nonlinear evolution of small-scale perturbations resulted in the reionization of the intergalactic medium at much lower redshifts. The fact that quasar spectra show an absence of an absorption trough from Ly α resonant scattering by neutral H atoms distributed diffusely along the line of sight, the Gunn-Peterson effect (Gunn & Peterson 1965), means that this reionization must have occurred with a high degree of efficiency before a redshift of 5.

One of the necessary consequences of this reionization is the presence of secondary anisotropies in the cosmic microwave background (CMB) due to the scattering of photons off ionized electrons. These secondary fluctuations can be divided into two classes: anisotropies due to nonlinear structures and linear anisotropies.

Nonlinear secondary anisotropies are of several types. Some of the more studied of these include the scattering of photons off the hot intracluster medium of galaxy clusters (Sunyaev & Zel’dovich 1970, 1972; or for more recent treatments see, e.g., Evrard & Henry 1991; Colfrancesco et al. 1994; Aghanim et al. 1997), gravitational lensing (see, e.g., Linder 1997; Metcalf & Silk 1997), the impact of inhomogeneous reionization (Aghanim et al. 1995; Peebles & Juszkievicz 1998; Knox, Scoccimarro, & Dodelson 1998), and the Rees-Sciama effect due to the bulk motions of collapsing nonlinear structures (see, e.g., Rees & Sciama 1968; Kaiser 1982; Seljak 1996).

Small-scale linear anisotropies come in fewer flavors. Detailed analyses of linear perturbations have uncovered a single dominant effect known as the Vishniac or Ostriker-Vishniac effect (Hu, Scott, & Silk 1994; Dodelson & Jubas 1995; Hu & White 1995; Hu & Sugiyama 1996). The level of these perturbations has been calculated by several authors (Ostriker & Vishniac 1985; Vishniac 1987; Jaffe & Kamionkowski 1998, hereafter JK).

These investigations raise the question of whether a detectable Vishniac effect even exists since nonlinear structures must exist on *some* length scale at the time of secondary scattering of CMB photons, as it is only by the formation of nonlinear objects that the universe is able to reionize itself. If these scales are comparable to those making the dominant contribution to the Vishniac effect, then a linear analysis is inappropriate and a calculation of secondary anisotropies must incorporate nonlinear effects.

In this work we determine the minimum length scale, R_V , which must remain linear in order for a linear approach to scattering by ionized regions with varying bulk motions to be accurate for the range of angular scales over which one can hope to measure secondary fluctuations. In hierarchical scenarios of structure formation, such as the Cold Dark Matter (CDM) model, smaller structures assemble at early times, later merging to form larger objects. This allows us to place limits on the time between the formation of structures large enough to reionize the universe and the time at which R_V becomes nonlinear. At that point, while peculiar velocities of ionized gas

continue to be imprinted on the microwave background, the nature of this signature is qualitatively different and is best interpreted from another perspective.

The structure of this work is as follows. In Sec. 2 we describe the Vishniac effect and determine the physical length scale on which it depends. In Sec. 3 we compare this to the scale of reionizing objects in different reionization scenarios and discuss the applicability of linear theory. In Sec. 4 we examine how the Vishniac effect is distinguished from other effects. Conclusions are given in Sec. 5, and the various cosmological expressions used throughout are summarized in the appendix.

2. Analysis

2.1. Approximations

The Vishniac effect is caused by the scattering of CMB photons by ionized regions with varying bulk motions. The temperature fluctuations induced along a line of sight are given by

$$\frac{\Delta T}{T}(\vec{\theta}) = - \int_0^{t_0} dt \sigma_T e^{-\tau(\vec{\theta}, t)} n_e(\vec{\theta}, t) \hat{\theta} \cdot \mathbf{v}(\vec{\theta}, t), \quad (1)$$

where $\tau(\vec{\theta}, t)$, $n_e(\vec{\theta}, t)$, and $\mathbf{v}(\vec{\theta}, t)$ are the optical depth along the line of sight, electron density, and bulk velocity, σ_T is the cross section for Thomson scattering, t is the age of the universe, and t_0 is the present age. Following JK, we choose a coordinate system in which $\hat{\theta}$ represents a three-dimensional unit vector along the line of sight, $\vec{\theta}$ represents a two-dimensional unit vector in the plane perpendicular to it, and bold letters represent fully three-dimensional vectors. Thus $\mathbf{v} = (v_x, v_y, v_z)$, $\vec{\theta} = (\theta_1, \theta_2, 0)$, and $\hat{\theta} = (\theta_1, \theta_2, \sqrt{1 - \theta_1^2 - \theta_2^2}) \approx (\theta_1, \theta_2, 1)$, the validity of the approximation deriving from the small-scale nature of the effect. Note that n_e , \mathbf{v} , and τ are all functions of position, the optical depth being given by $\tau(\vec{\theta}, t) = \int_t^{t_0} \sigma_T n_e(\vec{\theta}, t) c dt'$, where c is the speed of light.

If we decompose the density field into average and fluctuating components, we obtain, to leading order,

$$\frac{\Delta T}{T}(\vec{\theta}) = - \frac{\sigma_T n_0}{c} \int_0^1 dw a_0^3 \frac{x_e(\hat{\theta} w_{\text{ang}}, w)}{a(w)^2} (1 + \delta(\hat{\theta} w_{\text{ang}}, w) - \Delta\tau(\hat{\theta} w_{\text{ang}}, w)) \hat{\theta} \cdot \mathbf{v}(\hat{\theta} w_{\text{ang}}, w) e^{-\tau_0(w)}, \quad (2)$$

where $x_e(\mathbf{x}, w)$ is the ionization fraction, τ_0 and $\Delta\tau(\mathbf{x}, w)$ are the optical depths due to the average and fluctuating density components respectively, $a(w)$ is the scale factor with $a_0 \equiv a(0)$, $\delta(\mathbf{x}, w)$ is the overdensity field defined such that $\delta(\mathbf{x}, w) \equiv \rho(\mathbf{x}, w)/\bar{\rho}(w) - 1$ where $\rho(\mathbf{x}, w)$ is the density field and $\bar{\rho}(w)$ the average density as a function of comoving distance, n_0 is the present average electron density, and w_{ang} is the comoving angular distance, given by Eq. (27). Note that we have replaced time by w , the comoving distance defined by $dw \equiv c dt/a(t)$, and rewritten \mathbf{v} , and τ in comoving coordinates, \mathbf{x} . Taking the mass fraction of He to be $\sim 25\%$, and approximating helium

reionization as simultaneous to that of hydrogen, $n_0 = \Omega_b \rho_c / m_p \times 7/8 = 9.9 \times 10^{-6} \Omega_b h^2 \text{cm}^{-3}$, where ρ_c is the critical density, m_p is the mass of the proton, h is Hubble's constant normalized to $100 \text{ km s}^{-1} \text{ Mpc}^{-1}$, and Ω_b is the present baryonic matter density in units of the critical density.

The Vishniac effect arises by considering the homogeneously-reionizing, low optical depth case. In this case $x_e(\mathbf{x}, w)$ is independent of position and $\Delta\tau$ can be ignored. In practice, realistic reionization scenarios lead to low values of optical depth and hence dropping $\Delta\tau$ is a safe assumption (Hu, Scott, & Silk 1994). Indeed, the measurement of CMB fluctuations at large scales precludes the high degree of damping that would be caused by a high optical depth (Scott & White 1994; Hancock et al. 1998). The homogeneity of reionization, however, is a question of scales and thus represents a basic assumption on which the Vishniac analysis is based.

In this limit Eq. (2) becomes

$$\frac{\Delta T}{T}(\vec{\theta}) = - \int_0^1 dw g(w) \hat{\theta} \cdot \left(\mathbf{v}(\hat{\theta} w_{\text{ang}}, w) + \mathbf{q}(\hat{\theta} w_{\text{ang}}, w) \right), \quad (3)$$

where $\mathbf{q}(\mathbf{x}, t) \equiv \mathbf{v}(\mathbf{x}, w) \delta(\mathbf{x}, w)$ and $g(w)$ is the visibility function

$$g(w) \equiv \frac{a_0^3 n_0 x_e(w)}{c a(w)^2} \sigma_T e^{-\tau} = \frac{.121 \Omega_b h}{c} (1 + z(w))^2 x_e(w) e^{-\tau}, \quad (4)$$

with our conventions for the scale factor as in Appendix A. This gives the probability of scattering off reionized electrons and is a slowly-varying function of w .

Finally, we must approximate both \mathbf{v} and \mathbf{q} using linear theory. In this case, the density contrast at a comoving coordinate \mathbf{x} and comoving distance w from the observer is a random field with Fourier transform given by $\tilde{\delta}(\mathbf{k}, w) \equiv \int d^3\mathbf{x} \exp(-i\mathbf{k} \cdot \mathbf{x}) \delta(\mathbf{x}, w)$. The spatial and time dependence of $\tilde{\delta}(\mathbf{k}, w)$ can be factorized, so $\tilde{\delta}(\mathbf{k}, w) = \tilde{\delta}_0(\mathbf{k}) D(w) / D_0$ where $\tilde{\delta}_0(\mathbf{k}) \equiv \tilde{\delta}(\mathbf{k}, 0)$, $D(w)$ is the linear growth factor, given by Eq. (28), and $D_0 \equiv D(0)$. The power spectrum is then defined by the relation

$$\langle \tilde{\delta}_0(\mathbf{k}) \tilde{\delta}_0(\mathbf{k}') \rangle = \langle \tilde{\delta}_0(\mathbf{k}) \tilde{\delta}_0^*(-\mathbf{k}') \rangle = (2\pi)^3 \delta^3(\mathbf{k} + \mathbf{k}') P(k), \quad (5)$$

where $\delta^3(\mathbf{k} + \mathbf{k}')$ denotes the three-dimensional Dirac delta function. This completely specifies the probability density functional from which $\delta(\mathbf{k})$ is drawn in gaussian theories. In the CDM cosmogony, $P(k)$ is given by Eq. (31) and Eq. (33), and is dependent on the ‘shape parameter’ Γ , which is given as a function of cosmological parameters by Eq. (32) and constrained by observations of the galaxy correlation function to be $0.23^{+0.042}_{-0.034}$ (Viana and Liddle 1996). The overall normalization of $P(k)$ can be fixed by the amplitude of mass fluctuations on the $8 h^{-1} \text{ Mpc}$ scale as defined in Eq. (34).

The linear velocity field is simply related to the density field by the continuity equation $\nabla \cdot \mathbf{v}(\mathbf{x}) = -a(w) \dot{\delta}(\mathbf{x}, w)$ which in Fourier space gives

$$\tilde{\mathbf{v}}(\mathbf{k}, t) = \frac{ia(w)}{k^2} \frac{\dot{D}(w)}{D_0} \mathbf{k} \tilde{\delta}_0(\mathbf{k}), \quad (6)$$

where $\dot{D}(w)$ denotes the derivative of D with respect to time rather than w , and is given by Eq. (29). As the velocity always points along the direction of \mathbf{k} , only \mathbf{k} modes with large values along the line of sight can have large peculiar velocities in the $\hat{\theta}$ direction. But these modes are varying with wavelengths much smaller than variations in the window function and cancel when projected along the line of sight. It is only the second order (\mathbf{q}) term then, that contributes to the integral in Eq. (3).

A simple real-space argument gives a different way of understanding this cancellation. As gravitational perturbations to a pressureless fluid can be written in terms of the gradient of a scalar potential field ($\mathbf{v} \propto \nabla\phi$ where ϕ is the gravitational potential) the curl of the velocity field is zero to all orders. Thus a line integral of \mathbf{v} along a line of sight is approximately the integral of a gradient and is zero except for a small contribution at the end points. From all the terms in Eq. 2, only the $\delta \times \hat{\theta} \cdot \mathbf{v}$ survives to contribute to $\frac{\Delta T}{T}$.

2.2. Power Spectrum

Dropping the velocity term from Eq. 3, we can analytically construct the power spectrum of the angular fluctuations in the linear limit. Let us define $\frac{\tilde{\Delta T}}{T}(\vec{\kappa})$ as the Fourier transform of the temperature fluctuations such that $\frac{\tilde{\Delta T}}{T}(\vec{\kappa}) = \int d^2\vec{\theta} \exp(-i\vec{\kappa} \cdot \vec{\theta}) \frac{\Delta T}{T}(\vec{\theta})$, with the angular power spectrum defined as $P_{\text{ang}}(\kappa_1)(2\pi)^2\delta^2(\vec{\kappa}_1 + \vec{\kappa}_2) \equiv \langle \left(\frac{\tilde{\Delta T}}{T}(\vec{\kappa}_1) \frac{\tilde{\Delta T}}{T}(\vec{\kappa}_2) \right) \rangle$. At the small angular scales appropriate to the Vishniac effect, $P_{\text{ang}}(\kappa)$ is simply related to the usual C_ℓ s used to express CMB fluctuations by $C_\ell = P_{\text{ang}}(\kappa = \ell)$ (JK).

Several authors (Vishniac 1987; Kaiser 1992; JK) have derived expressions for the Vishniac C_ℓ s. Here we provide a new approach that, unlike other techniques, is easily extended to calculate higher-order moments, as is shown in §4. Our method is a simple extension of the usual formalism used to calculate single-point moments of the $\frac{\Delta T}{T}(\vec{\theta})$ distribution.

The simplest quantity of this sort is the second moment $\langle \left[\frac{\Delta T_B}{T}(0) \right]^2 \rangle$, where we use B to denote convolution with a beam profile. Given such a profile in Fourier space $B(\vec{\kappa})$, the second moment can be calculated as

$$\langle \left[\frac{\Delta T_B}{T}(0) \right]^2 \rangle = \int \frac{d^2\vec{\kappa}}{(2\pi)^2} B(\vec{\kappa})^2 P_{\text{ang}}(\kappa). \quad (7)$$

Suppose, however, that instead of asking about the second moment calculated from a single map observed with a beam $B(\vec{\kappa})$, we instead compute the single-point function as calculated from the convolution of two maps, observed by beams $B_1(\vec{\kappa})$ and $B_2(\vec{\kappa})$. As these profiles are arbitrary, we are free to take

$$B_1(\vec{\kappa}) \equiv (2\pi)^2\delta^2(\vec{\kappa} - \vec{\kappa}_1) \quad B_2(\vec{\kappa}) \equiv (2\pi)^2\delta^2(\vec{\kappa} - \vec{\kappa}_2), \quad (8)$$

where $\delta^2(\vec{\kappa})$ is the two-dimensional delta function. In this case we find

$$\langle \frac{\Delta T_{B_1}}{T}(0) \frac{\Delta T_{B_2}}{T}(0) \rangle = (2\pi)^2 P_{\text{ang}}(\kappa_1) \delta^2(\vec{\kappa}_1 + \vec{\kappa}_2), \quad (9)$$

recovering the angular power spectrum. Thus the power spectrum of the Vishniac effect can be computed from the single-point correlation if we are careful to express the beam profiles in sufficient generality.

Let us consider then

$$\langle \frac{\Delta T_{B_1}}{T}(0) \frac{\Delta T_{B_2}}{T}(0) \rangle = \int_0^1 dw_1 g(w_1) \int_0^1 dw_2 g(w_2) \int \frac{d^3 \mathbf{k}_a}{(2\pi)^3} \int \frac{d^3 \mathbf{k}_b}{(2\pi)^3} B_1(\vec{k}_a w_{1,\text{ang}}) B_2(\vec{k}_b w_{2,\text{ang}}) e^{i k_{a,z} w_1 + i k_{b,z} w_2} \langle \tilde{q}_z(\mathbf{k}_a, w_1) \tilde{q}_z(\mathbf{k}_b, w_2) \rangle, \quad (10)$$

where $\tilde{\mathbf{q}}(\mathbf{k}, w)$ is the Fourier transform of $\mathbf{q}(\mathbf{x}, w)$. Substituting in the expression for $\tilde{\mathbf{q}}$ in terms of $\tilde{\delta}$:

$$\tilde{\mathbf{q}}(\mathbf{k}, w) = \frac{ia(w) \dot{D}(w) D(w)}{D_0^2} \int \frac{d^3 \mathbf{k}'}{(2\pi)^3} \tilde{\delta}_0(\mathbf{k}') \tilde{\delta}_0(\mathbf{k} - \mathbf{k}') \frac{\mathbf{k}'}{k'^2}, \quad (11)$$

Eq. (10) becomes

$$\langle \frac{\Delta T_{B_1}}{T}(0) \frac{\Delta T_{B_2}}{T}(0) \rangle = - \int_0^1 dw_1 G(w_1) \int_0^1 dw_2 G(w_2) \prod_{j=1}^4 \left[\int \frac{d^3 \mathbf{k}_j}{(2\pi)^3} \right] B_1((\vec{k}_1 + \vec{k}_2) w_{1,\text{ang}}) B_2((\vec{k}_3 + \vec{k}_4) w_{2,\text{ang}}) e^{i(k_1+k_2)w_1 + i(k_3+k_4)w_2} \frac{k_{1,z}}{k_1^2} \frac{k_{3,z}}{k_3^2} \langle \prod_{l=1}^4 \tilde{\delta}_0(\mathbf{k}_l) \rangle, \quad (12)$$

where

$$G(w) \equiv \frac{g(w) a(w) D(w) \dot{D}(w)}{D_0^2}. \quad (13)$$

As $G(w)$ is slowly varying, we can follow Kaiser (1992) in dividing the integrals over comoving distance into N statistically independent intervals of width Δw , over each of which $G(w)$ is well approximated by a constant. In this case

$$\langle \frac{\Delta T_{B_1}}{T}(0) \frac{\Delta T_{B_2}}{T}(0) \rangle = - \sum_{n=1}^N G(w_n)^2 \Delta w^2 \prod_{j=1}^4 \left[\int \frac{d^3 \mathbf{k}_j}{(2\pi)^3} \right] B_1((\vec{k}_1 + \vec{k}_2) w_{n,\text{ang}}) B_2((\vec{k}_3 + \vec{k}_4) w_{n,\text{ang}}) j_0 \left(\frac{(k_{1,z} + k_{2,z}) \Delta w}{2} \right) j_0 \left(\frac{(k_{3,z} + k_{4,z}) \Delta w}{2} \right) \frac{k_{1,z}}{k_1^2} \frac{k_{3,z}}{k_3^2} \langle \prod_{l=1}^4 \tilde{\delta}_0(\mathbf{k}_l) \rangle. \quad (14)$$

As the density fluctuations are taken to be gaussian, we can expand the expectation value of the product of overdensities by Wick's theorem, keeping only the terms in which k_1 is paired with k_3 or k_4 . If we then define $k'_2 \equiv k_1 + k_2$, we find

$$\langle \frac{\Delta T_{B_1}}{T}(0) \frac{\Delta T_{B_2}}{T}(0) \rangle = \sum_{n=1}^N G(w_n)^2 \Delta w^2 \int \frac{d^3 \mathbf{k}_1}{(2\pi)^3} \int \frac{d^3 \mathbf{k}'_2}{(2\pi)^3} B_1(\vec{k}'_2 w_{n,\text{ang}}) B_2(-\vec{k}'_2 w_{n,\text{ang}}) \left[\frac{k_{1,z}^2}{k_1^4} + \frac{k_{1,z}(k'_{2,z} - k_{1,z})}{k_1^2 \|\mathbf{k}'_2 - \mathbf{k}_1\|^2} \right] P(k_1) P(\|\mathbf{k}'_2 - \mathbf{k}_1\|) j_0^2 \left(\frac{k'_{2,z} \Delta w}{2} \right). \quad (15)$$

The Bessel function has a width $\delta k_z \sim 1/\Delta w$ so $k_{2,z} \ll \kappa/w_{\text{ang}}$ wherever j_0^2 is appreciable. We can neglect terms that are smaller by a factor of $w_{\text{ang}}^2 \kappa^2 / \Delta w^2$ to obtain

$$\begin{aligned} \langle \frac{\Delta T_{B_1}}{T}(0) \frac{\Delta T_{B_2}}{T}(0) \rangle &= \sum_{n=1}^N G(w_n)^2 \Delta w \int \frac{d^3 \mathbf{k}_1}{(2\pi)^3} \int \frac{d^2 \vec{k}'_2}{(2\pi)^2} B_1(\vec{k}'_2 w_{\text{ang}}) B_2(-\vec{k}'_2 w_{\text{ang}}) \\ &\quad \frac{k_{1,z}^2}{k_1^4} - \frac{k_{1,z}^2}{k_1^2 ||(\vec{k}'_2, 0) - \mathbf{k}_1||^2} P(k_1) P(||(\vec{k}'_2, 0) - \mathbf{k}_1||). \end{aligned} \quad (16)$$

Taking

$$B_1(\vec{\kappa}) = B_2(\vec{\kappa}) = 2\pi\sigma^2 e^{-\frac{\sigma^2 \kappa^2}{2}} \quad (17)$$

gives the second moment as observed by a beam of gaussian width σ , while choosing beam profiles as given in Eq. (8) yields the angular power spectrum. In this case

$$C_\ell = P_{\text{ang}}(\kappa = \ell) = \int_0^1 dw \frac{G(w)^2}{w_{\text{ang}}^2} P_V(\ell/w_{\text{ang}}), \quad (18)$$

where

$$P_V(k) = \int \frac{d^3 \mathbf{k}_1}{(2\pi)^3} P(k') P(||(k, 0, 0) - \mathbf{k}_1||) \left[\frac{k_{1,z}^2}{k_1^4} - \frac{k_{1,z}^2}{k_1^2 ||(k, 0, 0) - \mathbf{k}_1||^2} \right], \quad (19)$$

which, choosing a coordinate system in which the z' axis points along the direction of $(k, 0, 0)$ becomes

$$P_V(k) = \frac{k}{8\pi^2} \int_0^\infty dx \int_{-1}^1 d\mu P(kx) P(k\sqrt{1-2x\mu+x^2})(1-\mu^2) \left[1 - \frac{x^2}{1-2x\mu+x^2} \right]. \quad (20)$$

This is equivalent to the usual expression for the Vishniac power spectrum

$$P_V(k) = \frac{k}{8\pi^2} \int_0^\infty dx \int_{-1}^1 d\mu P(kx) P(k\sqrt{1-2x\mu+x^2}) \frac{(1-\mu^2)(1-2x\mu)^2}{(1-2x\mu+x^2)^2}, \quad (21)$$

as can be seen by rewriting both integrals in rectangular coordinates and applying an origin shift. Thus the C_ℓ s are dependent on an integral along the line of sight of a term, $P_V(k)$, that is independent of redshift and arises from the convolution of the \mathbf{q} fields. We note in passing that our results are in agreement with Dodelson and Jubas (1995) and are twice the values found in JK.

2.3. Physical Scales

Having outlined the approximations which are used to calculate this effect and constructed the resulting power spectrum of fluctuations, we now examine which physical scales contribute most to $P_V(k)$. Typically, Eq. (18) is used to calculate the Vishniac effect by integrating over a particular matter power spectrum. To study the dependence of the effect on physical scale, we

replace the power spectrum that appears in Eq. (21) with $P(k)W^2(kR)$ where $P(k)$ is the CDM power spectrum and $W(x)$ is the spherical top-hat window function, given by Eq. (35). Here we consider a Λ CDM model in which the current nonrelativistic matter, vacuum, and baryonic densities in units of the critical density are $\Omega_0 = 0.35$, $\Omega_\Lambda = 0.65$, and $\Omega_b = 0.06$ respectively, and the “tilt” in the power spectrum as parameterized in Eq. (31) is taken to be flat, $n = 1.0$. If the other parameters are taken to be $h = 0.65$, $\sigma_8 = 1.05$, $\Gamma = 0.2$ and reionization occurs instantaneously and completely at $z_{\text{re}} = 18$, this results in $P_V(k)$ and C_ℓ as plotted in Fig. 1. Note that these values correspond to $\frac{\Delta T}{T}$ s a full order of magnitude smaller than large-scale primary anisotropies, pointing out the experimental challenges that must be overcome before secondary anisotropies can be measured (see, e.g., Subrahmanyam et al. 1993; Church et al. 1997). For reference we also plot the COBE-normalized primary fluctuations as computed by the CMBFAST code V2.4.1 (Seljak & Zaldarriaga 1996; Hu et al. 1998; Zaldarriaga & Seljak 1998), for the same cosmological model. Note that the position of this line is sensitive only to the Silk damping scale and thus is largely independent of the shape of the primordial power spectrum.

In this figure we see that even when filtered at the 1 Mpc/ h scale, the power spectrum is appreciably changed, especially at higher wavenumbers. While low ℓ fluctuations are not affected, a comparison with the solid line shows that these fluctuations are lost in the CMB primary signal and are very difficult to measure. Note that the damping shown in this graph represents not only a loss of power in linear theory, but also an increase of nonlinear power. Thus, at the point that the 1 Mpc/ h scale has become nonlinear, the Vishniac effect is competing with nonlinear effects over the range of angular scales in which it is able to be detected.

By the time the 2 Mpc/ h scale becomes nonlinear, however, the peak wavelength of the Vishniac effect has been shifted by a factor of 1/2 and $\sim 50\%$ of the power of $P_V(k)$ has been lost. At this point, linear calculations are unlikely to be reliable at measurable ℓ values $\gtrsim 4000$, and a more careful theoretical approach becomes necessary. These length scales are inversely proportional to the ‘shape parameter’ Γ which is 0.2 for this model. Thus we can conservatively fix $R_V = 2 \text{ Mpc}/h\Gamma_{0.2}$ where $\Gamma_{0.2} \equiv \Gamma/0.2$, as the maximum nonlinear length scale that still allows a linear analysis to be appropriate.

3. Redshift of applicability

Having determined R_V , we now consider what scenarios of reionization are compatible with a Vishniac effect. These scenarios can be roughly divided into two classes: those in which the dominant source of ionizing photons is due to stars formed in dwarf galaxies with halo masses $\gtrsim 10^6 M_\odot$ (Couchman & Rees 1986; Fukugita & Kawakasi 1994; Shapiro, Giroux, & Babul 1994; Haiman & Loeb 1997) and models in which reionization occurs due to active nuclei in galaxies with halo masses $\gtrsim 10^9 M_\odot$ (Efsthathiou & Rees 1988; Haehnelt & Rees 1993; Aghanim et al. 1995; Haiman & Loeb 1998; Valageas & Silk 1999). See also, however, the issues raised in Madau, Haardt, & Rees (1998) and Miralda-Escudé, Haehnelt, & Rees (1998), and the more exotic

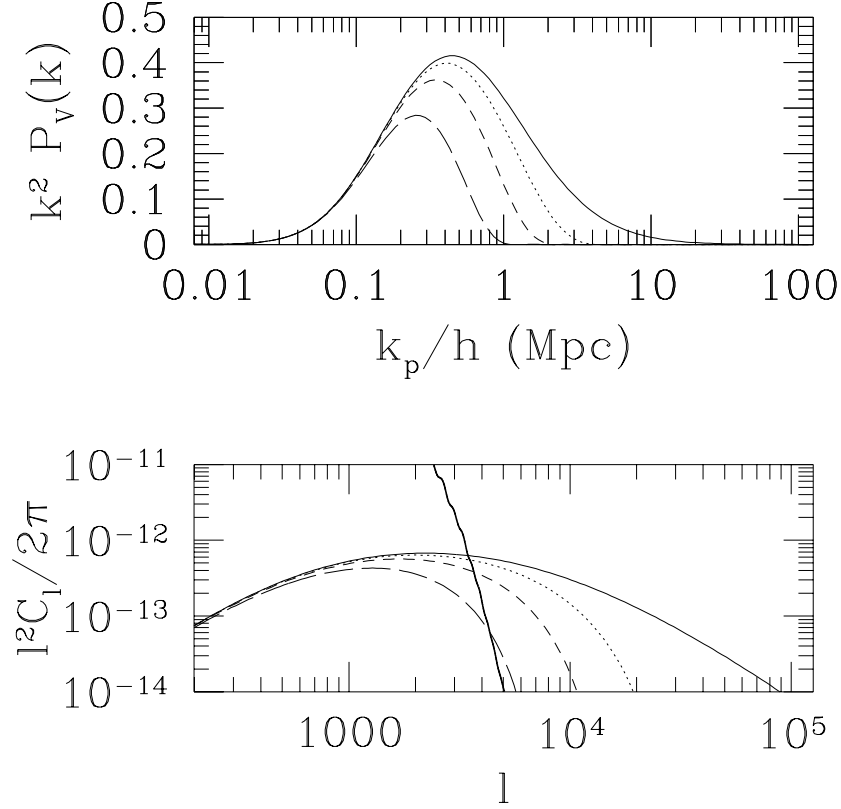


Fig. 1.— Upper panel: $P_V(k)$ from Λ CDM density fluctuations convolved with top-hat window functions of various scales. The solid line is the exact analytic expression, the dotted line corresponds to a top-hat filtering scale of $R = 1$ Mpc/h, the short-dashed to $R = 2$ Mpc/h, and the long dashed to $R = 4$ Mpc/h. The overall normalization is arbitrary as it is dependent on the choice of the scale factor. Lower panel: $\ell^2 C_\ell / 2\pi$ from density fluctuations convolved with top-hat window functions of various scales. Window functions are as in the upper panel. The sharply falling solid line shows the primary anisotropies as calculated by CMBFAST.

scenarios of reionization described in Scott, Rees, & Sciama (1991) and Adams, Sarkar, & Sciama (1998).

Models in which smaller objects are the most important predict redshifts of reionization of $z_{\text{re}} \approx 20$ while models in which reionization is due to objects on scales $\gtrsim 10^9 M_\odot$ predict more modest values of z_{re} . All models of reionization, however, are constrained by the lack of a Gunn-Peterson absorption trough in the spectra of high-redshift quasars, implying that the intergalactic medium was highly deficient in neutral hydrogen at redshifts $\lesssim 5$. Thus, high-mass reionization scenarios can only be successful in cosmologies in which the parameters are such that relatively large objects became nonlinear at high redshifts, precisely those models where the linear approximation is on the most shaky ground.

Using our value for R_V from Sec. 2, we are able to determine a redshift of applicability, z_V , below which the Vishniac approximation is invalid over the measurable range of ℓ scales. The number density of objects above a critical over-density, δ_c , is given by Press-Schechter theory (Press & Schechter 1974) as

$$\frac{dn(M, z)}{dM} = -\sqrt{\frac{2}{\pi}} \frac{\rho(z)}{M} \frac{\delta_c D_0}{\sigma(M)^2 D(z)} \exp\left(-\frac{\delta_c^2 D_0^2}{2\sigma^2(M) D(z)^2}\right) \frac{d\sigma}{dM}(M), \quad (22)$$

where $n(M, z)$ is the number density of collapsed objects per unit mass at a redshift of z , $\rho(z)$ is the comoving density of the universe at a redshift of z , $D(z)$ is the linear growth factor of fluctuations, and $\sigma(M)$ is the level of fluctuations on the mass scale corresponding to a sphere containing a mass M , which can be computed from Eq. (34). Typically, this formula is used to determine the number density of virialized halos. In this case $\delta_c(z)$ is a weak function of z for open models and Λ models and a fixed value of $3(12\pi)^{2/3}/20 \simeq 1.69$ in the $\Omega_0 = 1$ case (Kitayama & Suto 1996).

As a rough rule of thumb we can assume that reionization takes place when the 2σ fluctuations at the relevant scale have collapsed. In this case, $D(z_{\text{re}})/D_0 = \delta_c(z_{\text{re}})/(2\sqrt{2}\sigma(M))$ which is $\approx 0.6/\sigma(M)$ in the flat case. We take the linear approximation to be valid up the point at which the 1σ scale fluctuations at the R_V scale have reached an overdensity of 1. This gives $D(z_V)/D_0 = 1/(\sqrt{2}\sigma(R_V)) \approx 0.7/\sigma(R_V)$.

In Fig. 2 we plot both z_{re} and z_V as functions of mass, as it is the mass scale rather than the length scale that is most easily identified with different reionization scenarios. We consider three cosmologies, representative of parameters that favor both low mass-scale and high mass-scale scenarios of reionization. In order to compare with a scenario that is representative of stellar reionization, we consider a flat model normalized at the 8 Mpc/ h scale (Viana & Liddle 1996). Here $\Omega_0 = 1.0$, $\Omega_\Lambda = 0.0$, $\Omega_b = 0.07$, $h = 0.5$, $\sigma_8 = 0.60$, and $n = 1.0$. In this scenario $\Gamma = 0.44$, shifting the CDM line and decreasing R_V by a factor of ~ 2 . Note that this value of Γ is incompatible with the observed galaxy correlation function. Typical of high-mass reionization scenarios, we consider the “concordance model” of Ostriker & Steinhardt (1995), which was used by Haiman & Loeb (1998a) in their modeling of reionization by quasars. In this case the parameters

are taken to be $\Omega_0 = 0.35$, $\Omega_\Lambda = 0.65$, $\Omega_b = 0.04$, $h = 0.65$, $\sigma_8 = 0.87$, $\Gamma = 0.20$, and $n = 0.96$. Finally, we examine an open model with $\Omega_0 = 0.35$, again normalized at 8 Mpc/h. In this case $\Omega_\Lambda = 0.0$, $\Omega_b = 0.04$, $h = 0.65$, $\sigma_8 = 1.02$, $\Gamma = 0.20$, and $n = 1.0$.

Let us first consider the $\Omega_0 = 1$ model, represented by the lowest pair of lines. In this model σ_8 is the lowest of all the cosmologies considered and the perturbations evolve the most quickly. The combination of these two effects moves the redshift of applicability down to a value of $z_V \approx 2$, and thus one might expect to find an appreciable Vishniac effect. The problem, however, is that the low normalization and rapid evolution of perturbations also lowers the collapse redshift of the objects responsible for reionization. In this scenario, the 2σ , $10^9 M_\odot$ peaks collapse at $z_{\text{re}} \approx 7$. As reionization must have occurred with a high degree of efficiency by $z = 5$, this scenario is only marginally consistent with quasar absorption-line observations. Thus a flat cosmology is most compatible with low-mass reionization scenarios. If the collapse of $10^6 M_\odot$ halos is responsible for reionization, then $z_{\text{re}} \approx 13$ for this model, yielding a larger range of redshifts over which the Vishniac effect could be imprinted on the microwave background. This redshift is comparable to the revised values calculated in the stellar reionization scenario of Haiman and Loeb (1997; 1998b), although they consider a somewhat higher range of σ_8 values.

To quantify this further, in Figs. 3 and 4 we replot Fig. 2, replacing the vertical axis with $\int_0^{w(z)} dw G(w)^2 / w_{\text{ang}}^2 P_V(\ell/w_{\text{ang}})$, the contribution to C_ℓ due to bulk motions within a redshift of z . We take $\ell = 4000$ in Fig. 3 and $\ell = 12000$ in Fig. 4, and normalize the y axis such that the integral is equal to 1 at a redshift of $z_{\text{re}}(10^6 M_\odot)$. The magnitude of the Vishniac C_ℓ is then directly proportional to the vertical width of the gap between $\int_0^{w(z_{\text{res}})} dw G(w)^2 / w_{\text{ang}}^2 P_V(\ell/w_{\text{ang}})$, and $\int_0^{w(z_V)} dw G(w)^2 / w_{\text{ang}}^2 P_V(\ell/w_{\text{ang}})$, allowing us to judge the linear and nonlinear contributions to Eq. (18) in arbitrary scenarios of reionization at a glance.

From this point of view, reionization by $10^6 M_\odot$ objects results in only a marginal improvement the accuracy of a linear treatment. While 35% of the $\ell = 4000$ integral is nonlinear if $M_{\text{re}} = 10^9 M_\odot$, the $M_{\text{re}} = 10^6 M_\odot$ case is still 25% inaccurate. These numbers are somewhat lower in the high- ℓ case, in which 18% of the integral is nonlinear in the low mass case, and 25% in the high mass. Note however, that our definition of $R_V = 2 \text{ Mpc}(h\Gamma/0.2)$ was based on the damping of perturbations at $\ell = 4000$. From Fig. 1 we see that perturbations at $\ell = 12000$ are largely damped when the matter power spectrum is filtered at the $R = 1 \text{ Mpc}(h\Gamma/0.2)$ scale, and a more fair comparison between Figs. 3 and 4 would be to shift the vertical lines in Fig. 4 to masses lower by a factor of 8, yielding much the same numbers as in the $\ell = 4000$ case.

More typical of high-mass reionization scenarios is the Λ CDM model represented by the dotted lines in Figs. 2-4. In this model, σ_8 is slightly higher than in the flat case and the evolution of $D(z)$ is slowed. These effects raise the collapse redshift of $10^9 M_\odot$ peaks to $z_{\text{re}} \approx 11$, easily compatible with Gunn-Peterson tests. Note that our crude estimate of the redshift of reionization is almost the same as the redshift of ≈ 12 calculated by Haiman & Loeb (1998a) for the same set of cosmological parameters, using a more sophisticated Press-Schechter based argument for the

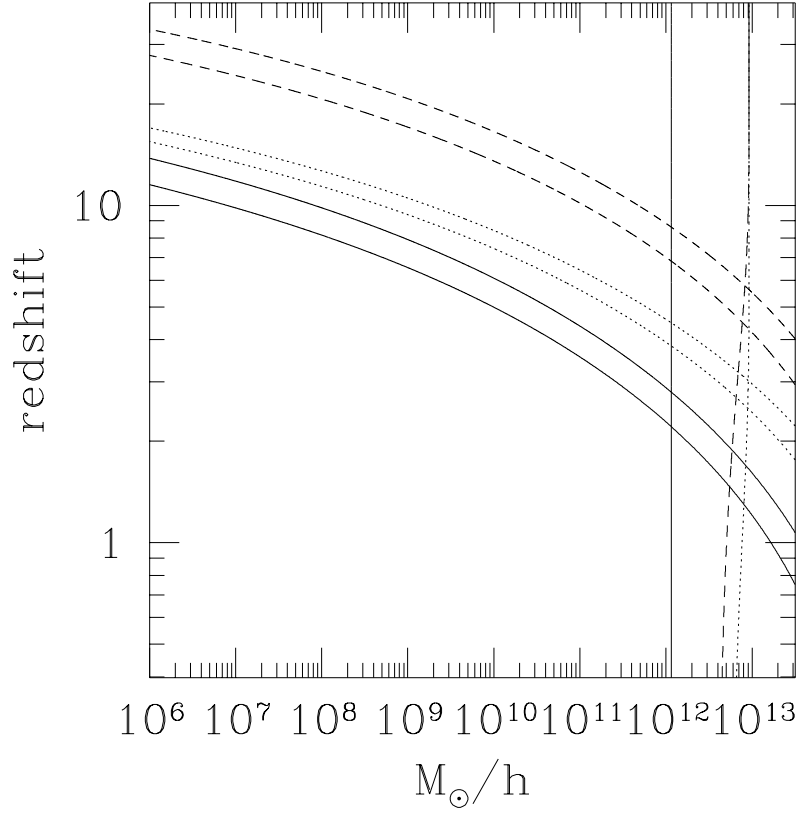


Fig. 2.— In each pair of horizontal lines the upper correspond to the ionization redshift $D(z_{\text{re}})/D_0 = \delta(z_{\text{re}})/(2\sqrt{2}\sigma(M))$, and the lower lines correspond to the redshift at which a linear treatment is no longer valid, $D(z_V)/D_0 = 1/(\sqrt{2}\sigma(M))$. The solid lines correspond to the flat model, the dotted lines to the “concordance model,” and the dashed lines to the open model, with parameters as described in the text. The nearly vertical lines show the mass scales corresponding to spheres of radius R_V for each of the models.

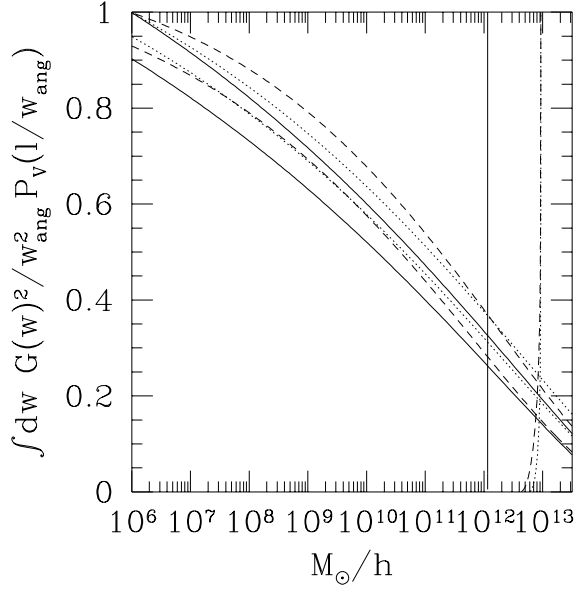


Fig. 3.— Fig. 2 replotted in terms of $\int_0^{w(z(M))} dw G(w)^2 / w_{\text{ang}}^2 P_V(\ell/w_{\text{ang}})$ with $\ell = 4000$ for three different cosmologies. Lines are as in Fig. 2.

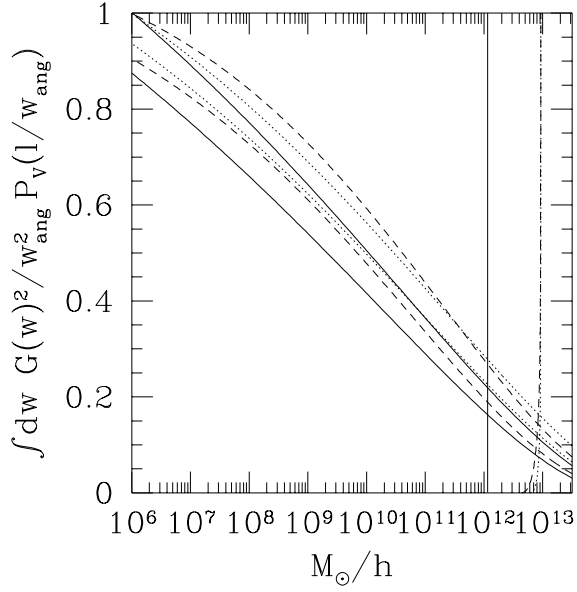


Fig. 4.— Same as Fig. 3 but with $\ell = 12000$. The onset of nonlinearity at the $R = 1 \text{ Mpc}(h\Gamma/0.2)$ scale can be estimated by shifting the nearly vertical lines to masses lower by a factor of 8.

ionizing flux from quasars. In this scenario z_V is also pushed back, although this is lessened by the shift of Γ as compared to the flat case. Thus $z_V \approx 2.5$.

One might imagine that in this case, a much wider margin of redshifts would lead to an accurate linear calculation. Fig. 3 indicates otherwise. In this case almost 20% of the low-mass and over 25% of the high-mass integral comes from redshifts at which R_V is nonlinear. The high- ℓ values are slightly lower, with 12% of the $10^6 M_\odot$ and 17% of the $10^9 M_\odot$ integral taking place when R_V is nonlinear, but again these numbers become roughly the same as the $\ell = 4000$ case for a more fair comparison.

The most extreme case we consider is the cluster-normalized open model, in which σ_8 is the highest and $D(z)$ the most slowly evolving. In this case $z_V \approx 4$, the $10^9 M_\odot$ and the $10^6 M_\odot$ schemes reionize at $z_{\text{re}} \approx 22$ and $z_{\text{re}} \approx 33$ respectively. This cosmology yields the largest regime of redshift space over which a linear analysis is valid and the most accurate results. Here nonlinear R_V scale fluctuations contaminate 15% of the low-mass and 20% of the high-mass C_{4000} integrals. Again these numbers are lower at higher ℓ but roughly the same after accounting for the smaller filtering scale of $R = 1 \text{ Mpc}(h\Gamma/0.2)$.

As a final check of the validity of our analysis, we construct $C_{\ell, \text{filtered}}$ defined as the angular power spectrum as given by Eq. (18) but replacing $P(k)$ with $P(k)W^2(kR_{\text{nl}}(z))$ where $R_{\text{nl}}(z)$ is now the nonlinear length scale *at each redshift* as in Fig. 2 ($D(z)/D_0 = 0.7/\sigma(R_{\text{nl}}(z))$). In Fig. 5 we plot the ratio of $C_{\ell, \text{filtered}}$ to C_ℓ calculated from the unfiltered CDM power spectrum. While only a few reionization scenarios are represented in this graph, this nevertheless gives us some feel of the accuracy of the linear treatment over different scales, and unlike Figs. 2 - 4, is completely independent of our definition of R_V . Here we see that in the range of ℓ values at which the effect is most likely to be measured ($4000 \lesssim \ell \lesssim 120000$) this estimate is in good agreement with the accuracies given in the previous figures. Note also that a linear treatment becomes increasingly inaccurate with ℓ , and thus measurements of fluctuations at angular scales just below this Silk damping scale will be most easy to interpret.

From these results we can safely conclude that even given our present ignorance as to the cosmological parameters, no more than $\approx 85\%$ of the contribution to Eq. (18) for measurable ℓ values can be calculated by linear theory in a CDM cosmogony. This depends only on the shape of the CDM power spectrum and the lack of diffuse $\text{L}\alpha$ absorption in quasar spectra out to $z \gtrsim 5$.

4. Is There a Detectable Vishniac Effect, Really?

At this point, one may raise the objection that our argument is a bit semantic, as there will still be scattering due to bulk motions even when linear theory breaks down. Indeed, the Kinetic Sunyaev-Zel'dovich effect, which is due to the peculiar velocities of clusters, can be viewed as a nonlinear counterpart to the Vishniac effect. Is there not, then, a sort of detectable Vishniac effect in cosmological scenarios in which R_V is nonlinear during the epoch of reionization, albeit under a

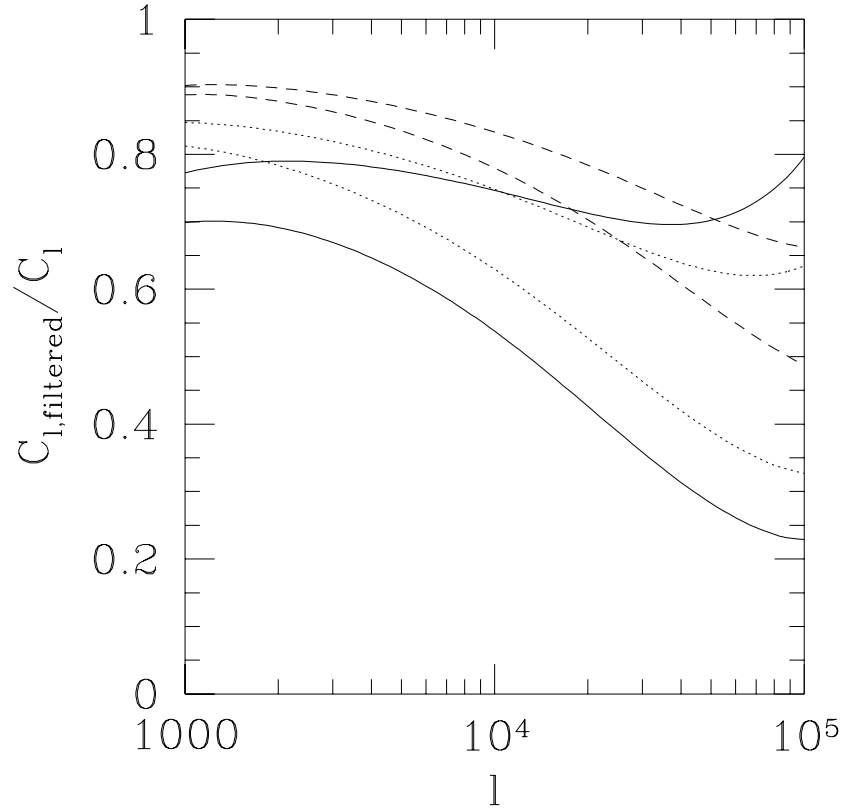


Fig. 5.— Ratio of the contribution to C_ℓ from the linear regime to the total calculated contribution as a function of ℓ . The solid lines correspond to the flat model, the dotted lines to the “concordance model,” and the dashed lines to the open model, and in each pair of lines the upper line corresponds to reionization by $10^6 M_\odot$ objects and the lower line to reionization by $10^9 M_\odot$ objects.

different name?

The problem with this point of view is that it overlooks some important physical distinctions between these effects. The Vishniac effect is due to the presence of a redshift regime in which $G(w)$ is slowly varying and a delicate cancellation takes place due to the lack of curl in the peculiar velocity field. As it can be calculated precisely, it provides a unique probe of the reionization history of the universe that is not available from measurements of nonlinear fluctuations.

Furthermore, the Vishniac effect displays a distinct signature of higher-order moments that allows it to be distinguished from other contributions. In order to understand why this occurs, let us consider the bispectrum $B(\vec{\kappa}_1, \vec{\kappa}_2)(2\pi)^2\delta^2(\vec{\kappa}_1 + \vec{\kappa}_2 + \vec{\kappa}_3) \equiv \langle \frac{\tilde{\Delta T}}{T}(\vec{\kappa}_1) \frac{\tilde{\Delta T}}{T}(\vec{\kappa}_2) \frac{\tilde{\Delta T}}{T}(\vec{\kappa}_3) \rangle$. We can apply our δ -function beam approach in the linear regime to calculate this as

$$\begin{aligned} \langle \frac{\tilde{\Delta T}}{T}(\vec{\kappa}_1) \frac{\tilde{\Delta T}}{T}(\vec{\kappa}_2) \frac{\tilde{\Delta T}}{T}(\vec{\kappa}_3) \rangle &= -i \prod_{i=1}^3 \left[\int_0^{w_0} dw_i G(w_i) \right] \prod_{j=1}^6 \left[\int \frac{d^3 \mathbf{k}_j}{(2\pi)^3} \right] \\ &(2\pi)^6 \delta^2((\vec{k}_1 + \vec{k}_2)w_{1,\text{ang}} - \vec{\kappa}_1) \delta^2((\vec{k}_3 + \vec{k}_4)w_{2,\text{ang}} - \vec{\kappa}_2) \delta^2((\vec{k}_5 + \vec{k}_6)w_{3,\text{ang}} - \vec{\kappa}_3) \\ &e^{i(k_{1,z}+k_{2,z})w_1+i(k_{3,z}+k_{4,z})w_2+i(k_{5,z}+k_{6,z})w_3} \frac{k_{1,z}}{k_1^2} \frac{k_{3,z}}{k_3^2} \frac{k_{5,z}}{k_5^2} \langle \prod_{l=1}^6 \tilde{\delta}_0(\mathbf{k}_l, w_l) \rangle. \end{aligned} \quad (23)$$

If $G(w)$ is slowly varying, we can again follow Kaiser (1992) in dividing the integrals over comoving distance into N statistically independent intervals of width Δw ,

$$\begin{aligned} \langle \frac{\tilde{\Delta T}}{T}(\vec{\kappa}_1) \frac{\tilde{\Delta T}}{T}(\vec{\kappa}_2) \frac{\tilde{\Delta T}}{T}(\vec{\kappa}_3) \rangle &= -i \sum_{n=1}^N G(w_n)^3 \Delta w^3 \prod_{j=1}^6 \left[\int \frac{d^3 \mathbf{k}_j}{(2\pi)^3} \right] (2\pi)^6 \delta^2((\vec{k}_1 + \vec{k}_2)w_{n,\text{ang}} - \vec{\kappa}_1) \\ &\delta^2((\vec{k}_3 + \vec{k}_4)w_{n,\text{ang}} - \vec{\kappa}_2) \delta^2((\vec{k}_5 + \vec{k}_6)w_{n,\text{ang}} - \vec{\kappa}_3) j_0 \left(\frac{(k_{1,z} + k_{2,z})\Delta w}{2} \right) \\ &j_0 \left(\frac{(k_{3,z} + k_{4,z})\Delta w}{2} \right) j_0 \left(\frac{(k_{5,z} + k_{6,z})\Delta w}{2} \right) \frac{k_{1,z}}{k_1^2} \frac{k_{3,z}}{k_3^2} \frac{k_{5,z}}{k_5^2} \langle \prod_{l=1}^6 \tilde{\delta}_0(\mathbf{k}_l, w_n) \rangle. \end{aligned} \quad (24)$$

As there are an odd number of k_z terms, there is no pairing of density fields that does not result in an odd k_z term. As all the k integrals are even, $\langle \frac{\tilde{\Delta T}}{T}(\vec{\kappa}_1) \frac{\tilde{\Delta T}}{T}(\vec{\kappa}_2) \frac{\tilde{\Delta T}}{T}(\vec{\kappa}_3) \rangle = 0$.

This cancellation can be understood from a more general perspective. $B(\vec{\kappa}_1, \vec{\kappa}_2)$ is generated by the expectation value of the triple product of the field \mathbf{q} . As \mathbf{q} is an isotropic vector field, $\langle \tilde{q}_i(\mathbf{k}_1) \tilde{q}_j(\mathbf{k}_2) \tilde{q}_k(\mathbf{k}_3) \rangle$ can depend on no vectors other than the \mathbf{k} vectors themselves and must therefore be proportional to at least one of the them (Monin & Yaglom 1971). This means that the $i = j = l = z$ component of this product must be proportional to $k_{1,z}$, $k_{2,z}$, or $k_{3,z}$. Thus the odd k_z term that results in $B(\vec{\kappa}_1, \vec{\kappa}_2) = 0$ is due to the isotropy of the density fluctuations. By a similar argument, all odd moments of the temperature fluctuations must be zero as these also depend on the expectation value of the product of an odd number of \mathbf{q} 's. Note that this is true independent of the gaussianity of the probability distribution functional of $\tilde{\delta}(\mathbf{k})$.

This cancellation does not apply to the even moments, however, as an even number of \mathbf{q} 's can be arranged in a way that is not proportional to one of the \mathbf{k} vectors. Thus the Vishniac

effect is unique in that it is nongaussian independent of the gaussianity of the probability distribution functional of $\tilde{\delta}(\mathbf{k})$, but this nongaussianity is expressed only in the even higher-order moments. This alternation of zero-and-nonzero higher-order moments provides a unique signal that distinguishes the Vishniac effect from other secondary anisotropies, and provides us with the opportunity to use nongaussian statistics as a discriminator between these contributions. Note however, that the difficulty of measuring secondary anisotropies may make such an analysis difficult to apply in practice.

5. Conclusions

Due to the tremendous predictive power of linear theory, comparisons between linear predictions and large-scale cosmic microwave background measurements promise to constrain cosmological parameters to the order of a few percent (Jungman et al. 1996; Bond, Efstathiou, & Tegmark 1997; Zaldarriaga, Spergel, & Seljak 1997). The natural extension of this approach is to try to measure small-scale secondary anisotropies and match them to linear predictions to study the reionization history of universe. The situation in this case is more muddled, however, as a number of nonlinear secondary effects also contribute at these scales.

The dominant secondary linear anisotropy is a second-order contribution known as the Vishniac or Ostriker-Vishniac effect. As this effect can be predicted accurately as a function of cosmological parameters, several authors have proposed that its measurement will prove to be a sensitive probe of the reionization history of the universe. Reionization occurs by the formation of nonlinear structures, however, raising the question of whether a regime of redshift space exists in which these objects have collapsed but a linear analysis is still appropriate.

In this work, we have determined the relevant physical scales that give rise to the Vishniac effect in a Cold Dark Matter cosmogony, showing that approximations are already compromised when $1 \text{ Mpc}/(h\Gamma_{0.20})$ scales have become nonlinear, and break down when $2 \text{ Mpc}/(h\Gamma_{0.20})$ dark matter halos reach overdensities of 1. The width of the redshift regime over which the effect can be imprinted on the CMB is dependent on the cosmological parameters and the reionizing mass scale. Schemes in which reionization is due to radiation from active galactic nuclei associated with dark matter halos of masses $\gtrsim 10^9 M_\odot$ are limited by the absence of a Gunn-Peterson absorption trough. As reionization must have occurred with a high degree of efficiency before a redshift of 5, such models are successful only if one assumes a large value of σ_8 , or considers open models with slowly-changing linear growth factors. Both these assumptions push back the redshift at which R_V becomes nonlinear, limiting the range over which a linear analysis is appropriate.

Scenarios in which reionization is due to much smaller objects, such as stars formed in dwarf galaxies associated with dark matter halos of masses $\gtrsim 10^6 M_\odot$, are able to reionize the universe at much larger redshifts even in cosmologies in which σ_8 is small and $D(z)$ quickly evolving. This represents only a marginal gain however, as the high redshift contribution to the Vishniac integral

is roughly proportional to comoving distance, and comoving distances are small at high redshifts. Thus low-mass scenarios of reionization are more compatible with a linear analysis not so much because they reionize earlier as because they allow R_V to become nonlinear more recently without violating Gunn-Peterson limits.

The Vishniac effect arises from physical processes that are distinct from nonlinear secondary anisotropies. Its detection indicates the presence of a redshift regime in which a delicate cancellation takes place due to the lack of curl in the peculiar velocity field and slow variations in $G(w)$. This leaves a unique signature in the higher-order moments of the temperature fluctuations that is absent from its nonlinear counterparts. Furthermore, due to the predictive power of linear theory, it represents a sensitive probe of the reionization history not available from measurements of nonlinear contributions.

As with measurements of large angular scale anisotropies, small-scale microwave background anisotropy measurements have the potential to uncover much about the history of our universe. Also as with large-scale measurements, whether this potential will be realized remains to be seen. While the Vishniac effect represents a possible probe of the reionization epoch, the analysis will, as always, be more involved than first suggested. Ultimately it will only be through the measurement and analysis of small-scale microwave background anisotropies that we will be able to know if there is a detectable Vishniac effect.

I wish to thank Nabila Aghanim, François Bouchet, Rychard Bouwens, Andrew Jaffe, Douglas Scott, and Naoshi Sugiyama for helpful discussions and am particularly indebted to Joseph Silk, whose comments and suggestions have been invaluable during the preparation of this work. I thank Uroš Seljak and Matias Zaldarriaga for the use of CMBFAST and acknowledge partial support by the NSF.

Appendix

In this appendix, we provide explicit expressions for the cosmological factors used throughout this paper. We allow both Ω_0 and Ω_Λ to be free. In this case the Friedman equations for the evolution of the scale factor of the Universe, $a(z)$ are

$$\frac{\dot{a}}{a} = H_0 E(z) \equiv H_0 \sqrt{\Omega_0(1+z)^3 + \Omega_\Lambda + (1 - \Omega_0 - \Omega_\Lambda)(1+z)^2}, \quad (25)$$

and

$$\frac{\ddot{a}}{a} = H_0^2 [\Omega_\Lambda - \Omega_0(1+z)^3/2], \quad (26)$$

where $H_0 = 100 h \text{ km sec}^{-1} \text{ Mpc}^{-1}$ is the Hubble constant, and the overdot denotes a derivative with respect to time.

We choose the scale factor such that $a_0 H_0 = 2c$. If we are located at the origin, $w = 0$, then an object at redshift z is at a comoving distance, $w(z) = \frac{1}{2} \int_0^z dz' E^{-1}(z')$ and at a time $t(z) = \frac{1}{H_0} \int_z^\infty dz' (1+z')^{-1} E^{-1}(z')$. Note that this is different than conformal time, defined by $d\eta = dt/a$, such that $c\eta(z) = w(\infty) - w(z)$. For any flat universe the angular size distance $w_{\text{ang}} = w$, and in an open universe

$$w_{\text{ang}} = \frac{\sinh(2w\sqrt{1-\Omega_0-\Omega_\Lambda})}{2\sqrt{1-\Omega_0-\Omega_\Lambda}}. \quad (27)$$

The growth factor as a function of redshift is

$$D(z) = \frac{5\Omega_0 E(z)}{2} \int_z^\infty \frac{1+z'}{[E(z')]^3} dz', \quad (28)$$

while

$$\frac{\dot{D}}{D} = \frac{\ddot{a}}{\dot{a}} - \frac{\dot{a}}{a} + \frac{5\Omega_0}{2} \frac{\dot{a}}{a} \frac{(1+z)^2}{[E(z)]^2 D(z)}. \quad (29)$$

The evolution of Ω is given by

$$\Omega(z) = \Omega_0(1+z)^3 E^{-2}(z) \quad (30)$$

where $\Omega_0 = \Omega(0)$.

For the power spectrum, we use

$$P(k) = \frac{2\pi^2}{8} \delta_H^2 (k/2)^n T^2(k_p \text{ Mpc}/h\Gamma), \quad (31)$$

where $T(q)$ is the CDM transfer function, $k_p = k/a_0 = kH_0/2c$ is the physical wavenumber, and the shape parameter Γ is defined as (Sugiyama 1995)

$$\Gamma \equiv \Omega_0(h/0.5) \exp(-\Omega_b - \Omega_b/\Omega_0). \quad (32)$$

The factor of 8 in the denominator in Eq. (31) arises because we are using $a_0 H_0 = 2c$. For the transfer function, we use the analytic fit given by Bardeen et al. (1986) for the CDM cosmogony,

$$T(q) = \frac{\ln(1 + 2.34q)/(2.34q)}{[1 + 3.89q + (16.1q)^2 + (5.46q)^3 + (6.71q)^4]^{1/4}}. \quad (33)$$

The normalization factor δ_H can be fixed by specifying $\sigma(8\text{Mpc}/h)$, where the variance of the mass enclosed in a sphere of radius R is given by

$$\sigma^2(R) = \frac{1}{2\pi^2} \int_0^\infty k^2 dk P(k) W^2(k_p R). \quad (34)$$

Here $W(x)$ is the spherical top-hat window function, defined in Fourier space as

$$W(x) \equiv 3 \left[\frac{\sin(x)}{x^3} - \frac{\cos(x)}{x^2} \right]. \quad (35)$$

REFERENCES

- Adams, J. A., Sarkar, S., & Sciamma, D. W. 1998, MNRAS, 301, 210
- Aghanim, N., De Luca, A., Bouchet, F. R., Gispert, R., & Puget, J. L. 1997, A&A, 325, 9
- Aghanim, N., Désert, F. X., Puget, J. L., & Gispert, R. 1995, A&A, 331, 1
- Bardeen, J. M., Bond, J. R., Kaiser, N., & Szalay, A. 1986, ApJ, 304, 15
- Bond, J. R., Efstathiou, G., & Tegmark, M. 1997, 291, 33
- Bunn, E. F., & White, M. 1997, ApJ, 480, 6
- Church, S. E., Ganga, K. M., Ade, P. A. R., Holtzapfel, W. L., Mausekopf, P. D., Wilbanks, T. M., & Lange, A. E. 1997, ApJ, 484, 523
- Colafrancesco, S., Mazzotta, P., Rephaeli, Y., & Vittorio, N. 1994, ApJ, 433, 454
- Couchman, H. M. P., & Rees, M. J. 1986, MNRAS, 221, 53
- Dodelson, S., & Jubas, J. M. 1995, ApJ, 439, 503
- Efstathiou, G., Rees, M. J. 1998, MNRAS, 230, 5
- Evrard, A. E., & Henry, J. P. 1991, ApJ, 383, 95
- Fukugita, M., & Kawasaki, M. 1994, MNRAS, 269, 563
- Gunn, J. E., & Peterson, B. A. 1965, ApJ, 142, 1633
- Haehnelt, M. G., & Rees, M. J. 1983, MNRAS, 263, 168
- Hancock, S., Rocha, A., Lasenby, N., & Gutierrez, C. M. 1998, MNRAS, 294, L1
- Haiman, Z., & Loeb, A. 1997, ApJ, 483, 21
- Haiman, Z., & Loeb, A. 1998a, ApJ, 503, 505
- Haiman, Z., & Loeb, A. 1998b, ApJ, 499, 520
- Hu, W., Scott, D., & Silk, J. 1994, Phys. Rev. D, 49, 648
- Hu, W., Seljak, U., White, M., & Zaldarriaga, M. 1998, Phys. Rev. D, 57, 3290
- Hu, W., & Sugiyama, N. 1996, ApJ, 471, 542
- Hu, W., & White, M. 1995, A&A, 315, 33
- Jaffe, A. H., & Kamionkowski, M. 1998, Phys. Rev. D, 58, 43001 (JK)
- Jungman, G., Kamionkowski, M., Kosowsky, A., & Spergel, D. N. 1996, Phys. Rev. D, 54, 1332
- Kaiser, N. 1982, MNRAS, 198, 1033
- Kaiser, N. 1992, ApJ, 388, 272
- Kitayama, T., & Suto Y. 1996, ApJ, 469, 480
- Knox, L., Scoccimarro, R., & Dodelson, S. 1998, Phys. Rev. Lett, 81, 2004
- Linder, E. V. 1997, A&A, 323, 305
- Madau, P., Haardt, F., & Rees, M. H. 1999, ApJ, 514, 648
- Metcalf, R. B., & Silk, J. 1997, ApJ, 489, 1
- Miralda-Escudé, J., Haehnelt, M., & Rees, M. J. 1998, submitted to ApJ (astro-ph/9812306)
- Monin, A. S., & Yaglom, A. M. 1971, Statistical Fluid Mechanics, Volume 2 (Cambridge: MIT Press)
- Ostriker, J. P., & Steinhart, P. J. 1995, Nature, 377, 600

- Ostriker, J. P., & Vishniac, E. T. 1985, ApJ, 306, L51
- Peebles, P. J. E., Juskiewicz, R. 1998, ApJ, 509, 483
- Press, W. H., & Schechter, P. L. 1974, ApJ, 187, 425
- Rees, M. J., & Sciama, D. W. 1968, Nature, 517, 611
- Scott, D., Rees, M. J., & Sciama, D. W. 1991, A&A, 250, 295
- Scott, D., & White, M. 1994, in Proc. of the CWRU CMB Workshop, “Two years after COBE” eds. L. Krauss, & P. Kernan
- Seljak, U. 1996, ApJ, 460, 549
- Seljak, U. & Zaldarriaga, M. 1996, ApJ 469, 437
- Subrahmanyan, R., Ekers, R. D., Sinclair, M., & Silk, J. 1993, MNRAS, 263, 416
- Sugiyama, N. 1995, ApJS, 100, 281
- Sunyaev, R. A., & Zel’dovich, Ya. B. 1970, Ap&SS, 7, 3
- Sunyaev, R. A., & Zel’dovich, Ya. B. 1972, Comments Astrophys. Space Phys., 4, 173
- Shapiro, P. R., Giroux, M. L., & Babul, A. 1994, ApJ, 427, 25
- Valageas P., & Silk, J. 1999, A&A, 347, 1
- Viana, P. T. P., & Liddle, A. 1996, MNRAS, 281, 323
- Vishniac, E. T. 1987, ApJ, 332, 597
- Zaldarriaga, M., & Seljak, U. 1998, Phys. Rev. D, 58, 23003
- Zaldarriaga, M., Spergel, D. N., & Seljak, U. 1997, ApJ, 488, 1